Comparing drifter and altimeter-derived velocities in the Southern Ocean

Shane Elipot Sarah Gille selipot@ucsd.edu sgille@ucsd.edu
Scripps Institution of Oceanography, University of California, San Diego, La Jolla, CA

1. Introduction

► Our primary goal is to study the wind-driven surface circulation of the Southern Ocean as rendered by drifter data. Using altimeter data helps distinguish the surface circulation driven by *local* wind forcing from the large-scale and mesoscale pressure-driven geostrophic circulation.

► The drifter velocity can be decomposed into a geostrophic and an ageostrophic component:

$$\mathbf{U}_{\text{drifter}} = \mathbf{U}_{\text{geostrophic}} + \mathbf{U}_{\text{ageostrophic}} + \text{Noise} = \mathbf{U}_{\text{geostrophic}} + \mathbf{U}_{\text{Ekman}} + \mathbf{U}_{\text{wind-slip}} + \text{Noise}$$

► We examine the importance of the geostrophic and ageostrophic components as a function of frequency.

2. Data and Methods

► 10,431 40-day time series of drifter position and velocity were obtained from a total of 875 drifter trajectories collected over a 13 year period as part of the WOCE Surface Velocity Program. Time series overlap by 20-days. These segments were binned in 2° latitude bands. The individual trajectories (a) and the distribution (b) of the segments' mean latitude are plotted.

► Merged T/P-ERS maps of sea level anomalies from AVISO at 7-day intervals are used to derive geostrophic current anomalies at the surface. A mean sea level from hydrography [*Gouretski and Jancke, 1998*] and hence a mean sea surface geostrophic velocity is added. Geostrophic velocities were interpolated in time and space at each drifter location.

► Ageostrophic velocities are estimated by subtracting geostrophic velocities from drifter velocities.

► ECMWF 10-m wind fields at 6-hour intervals are used to derive wind stress at the ocean surface [*Smith, 1980*]. The wind stress is interpolated in time and space at the drifter locations.

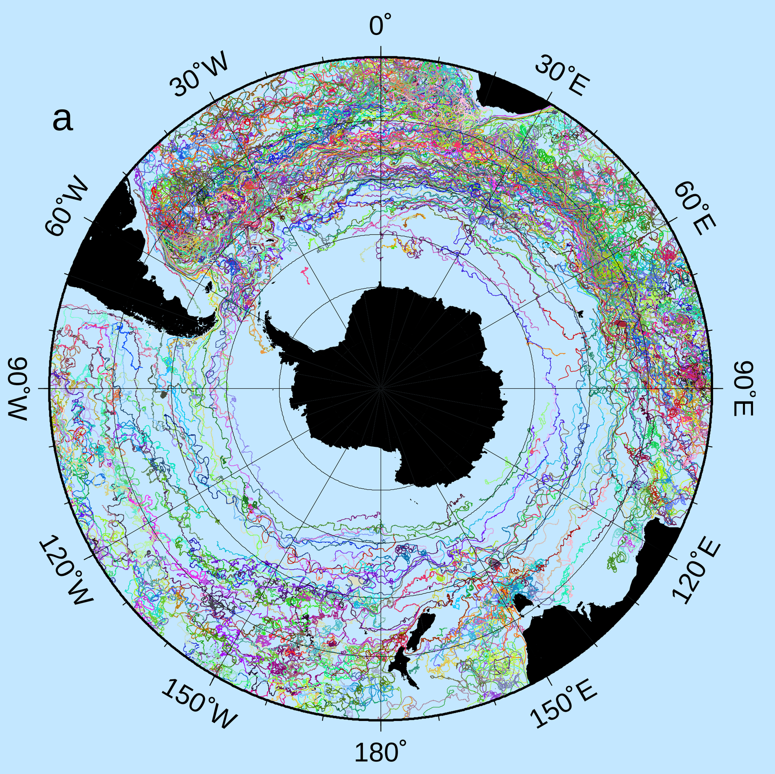

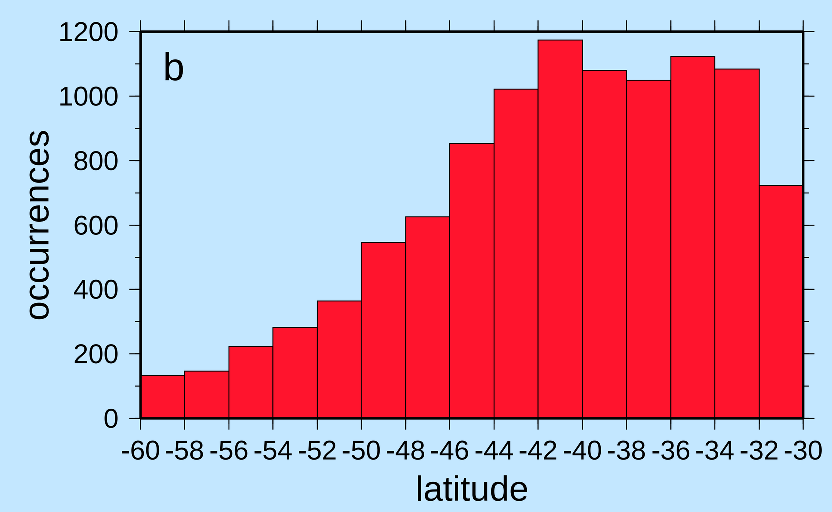

► **Spectral analysis**

For a vector time series $\mathbf{U}$, the normalized spectrum is:

$$S(\nu^{\pm}) = \left\langle \tilde{\mathbf{U}}\tilde{\mathbf{U}}^{*} \right\rangle / \nu_r,$$

where $\tilde{\cdot}$ designates the Fourier transform, * the complex conjugate and $\langle\cdot\rangle$ the ensemble average. ν_r =1/40 cpd is the frequency resolution for this study.

► For the Southern Hemisphere positive frequencies correspond to anticyclonic motions and negative frequencies to cyclonic motions. The two types of motions add and form an ellipse in each frequency band.

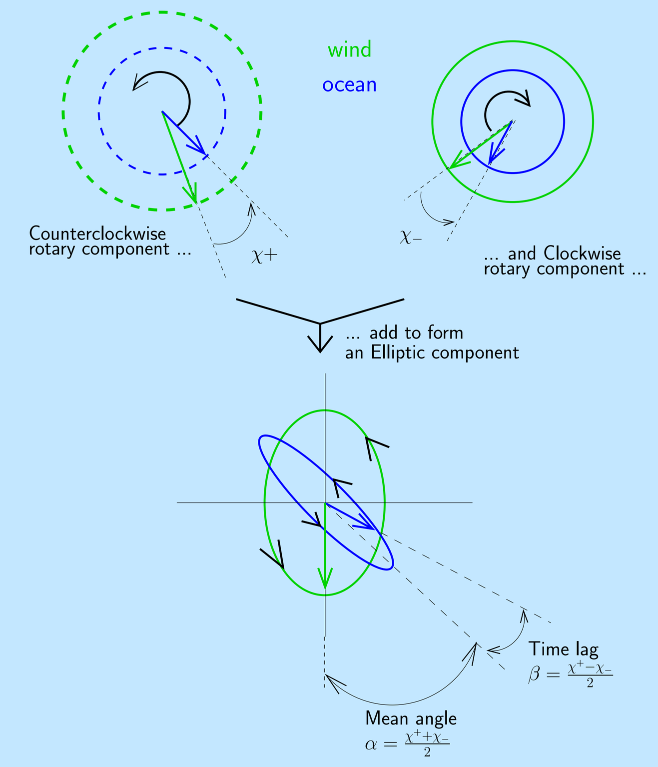

► **The Rotary Coefficient**

$$r = \frac{S(\nu^+) - S(\nu^-)}{S(\nu^+) + S(\nu^-)}$$

represents the partition of power between anticyclonic (+) and cyclonic (-) motions.

► **Cross-Spectral analysis**

The **coherence squared** γ^2 and the **coherence phase** χ between two vector time series $\mathbf{U}_1$ and $\mathbf{U}_2$ are:

$$\gamma^2(\nu^{\pm}) = \frac{\left|\left\langle \tilde{\mathbf{U}}_1\tilde{\mathbf{U}}_2^{*}\right\rangle\right|^2}{\left\langle \tilde{\mathbf{U}}_1\tilde{\mathbf{U}}_1^{*}\right\rangle \left\langle \tilde{\mathbf{U}}_2\tilde{\mathbf{U}}_2^{*}\right\rangle}, \quad \chi(\nu^{\pm}) = \arctan\left[\frac{\mathcal{I}\left(\left\langle \tilde{\mathbf{U}}_1\tilde{\mathbf{U}}_2^{*}\right\rangle\right)}{\mathcal{R}\left(\left\langle \tilde{\mathbf{U}}_1\tilde{\mathbf{U}}_2^{*}\right\rangle\right)}\right].$$

Our convention is such that a positive phase means that $\mathbf{U}_1$ is to the left of $\mathbf{U}_2$.

3. Spectral comparison

► **Power Spectral Density of drifter velocities (left panels).** The maximum errorbar for the whole domain is shown as a box on the colorscale.
► The anticyclonic spectrum (upper panel) shows the inertial peak at $\nu = f$.

► **Power Spectral Density of geostrophic velocities (right panels).** The maximum errorbar for the whole domain is shown as a box on the colorscale .
► The geostrophic spectra are less energetic than the drifter spectra.

► **Rotary Coefficient** of drifter (left panel) and geostrophic (right panel) velocities. Gray areas correspond to non statistically significant polarization at the 95% level.
► The drifter spectra show a strong anticyclonicity in the inertial band (1 to 2 cpd) and some cyclonicity in the 0.1 to 1 cpd frequency bands.
► The geostrophic spectra show a strong cyclonicity which decreases with latitude.

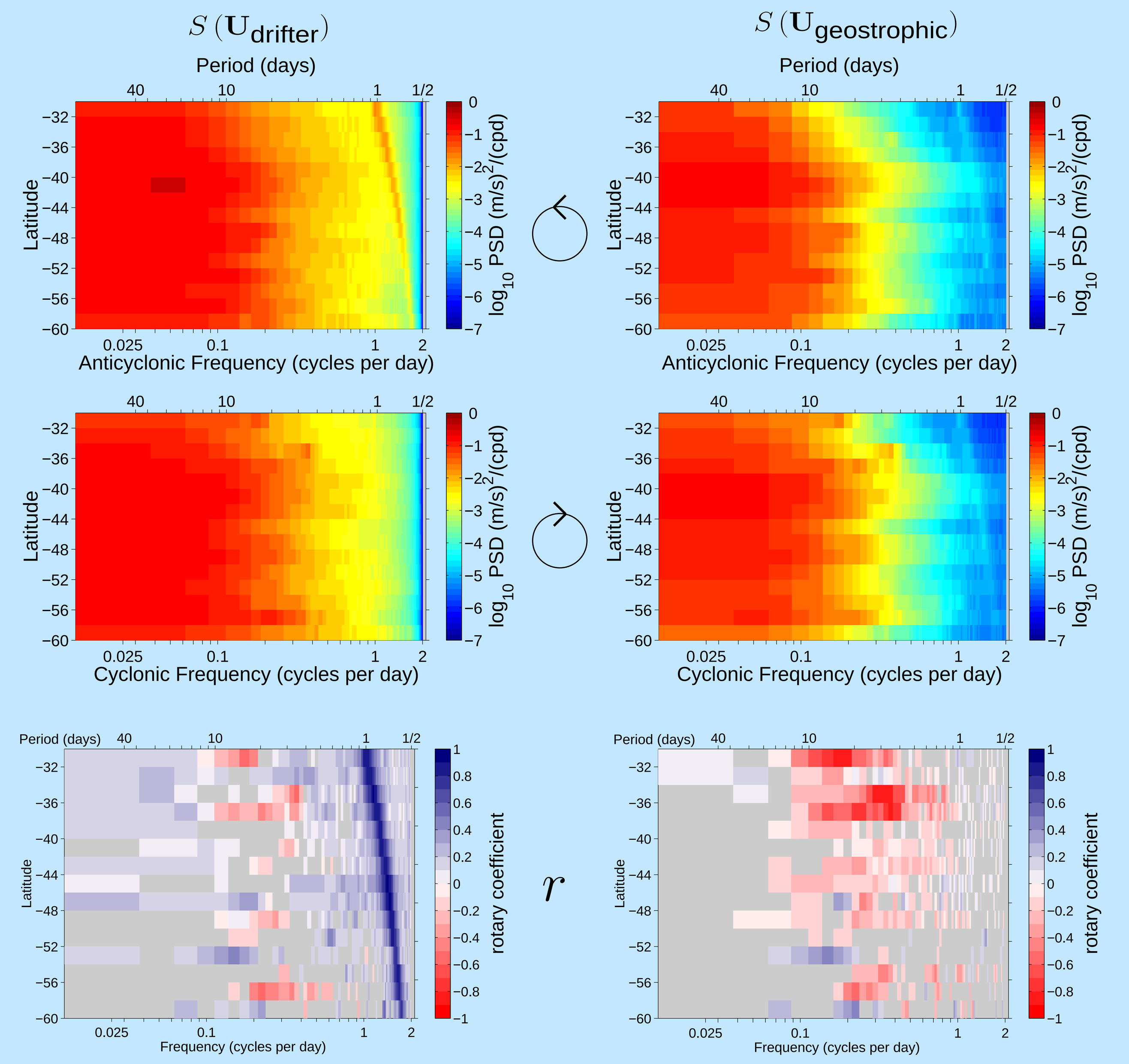

4. The geostrophic component

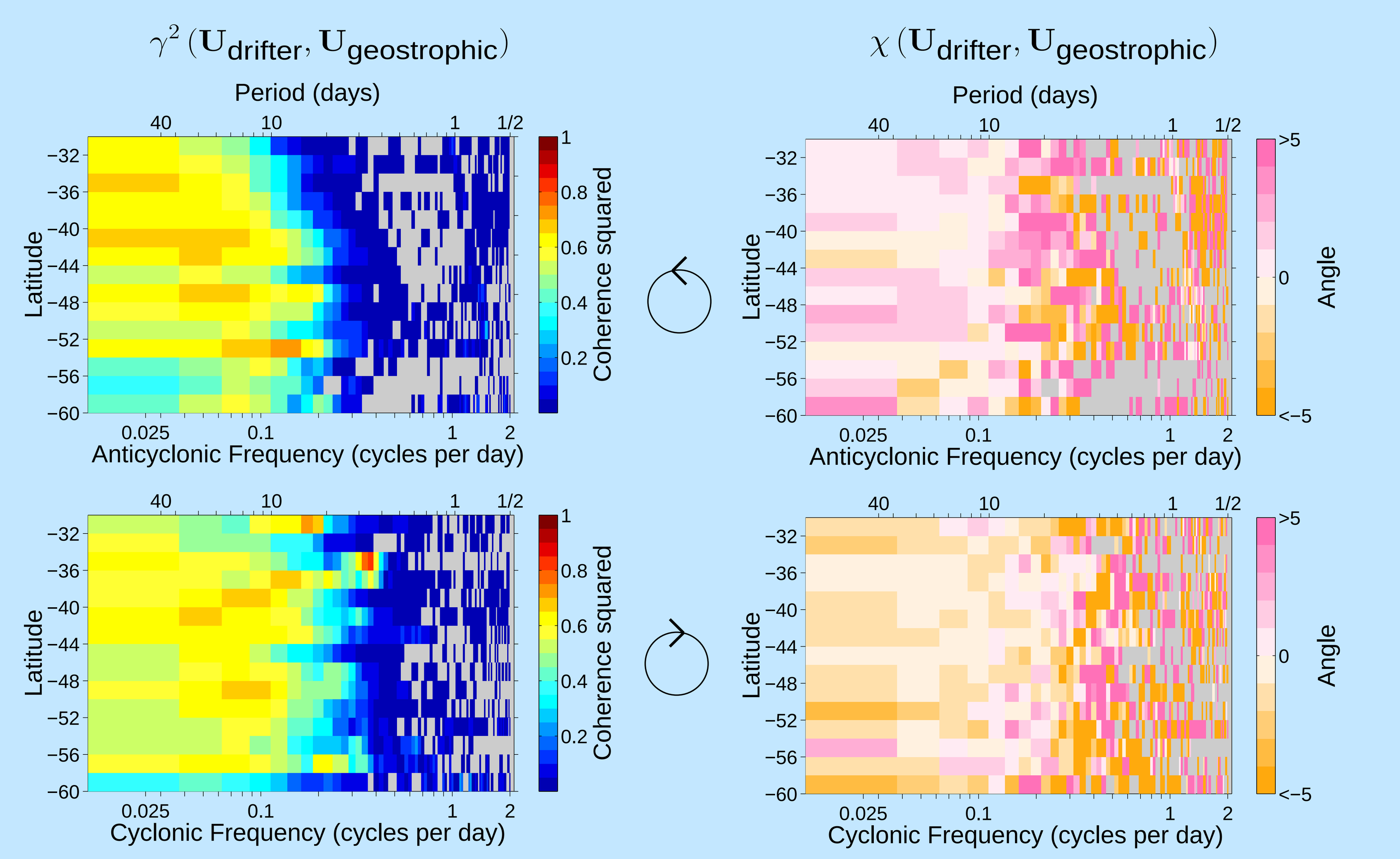

► **Coherence Squared** and **Coherence Phase** between $\mathbf{U}_{\text{drifter}}$ and $\mathbf{U}_{\text{geostrophic}}$ for anticyclonic frequencies (top panels) and cyclonic frequencies (lower panels). Gray areas correspond to non statistically significant coherence squared at the 95% level.
► Up to the altimeter Nyquist frequency (1/14 cpd), the geostrophic velocities explain up to 60% of the drifter variance. For these frequency bands, the phase is less than 5°.

5. The ageostrophic component

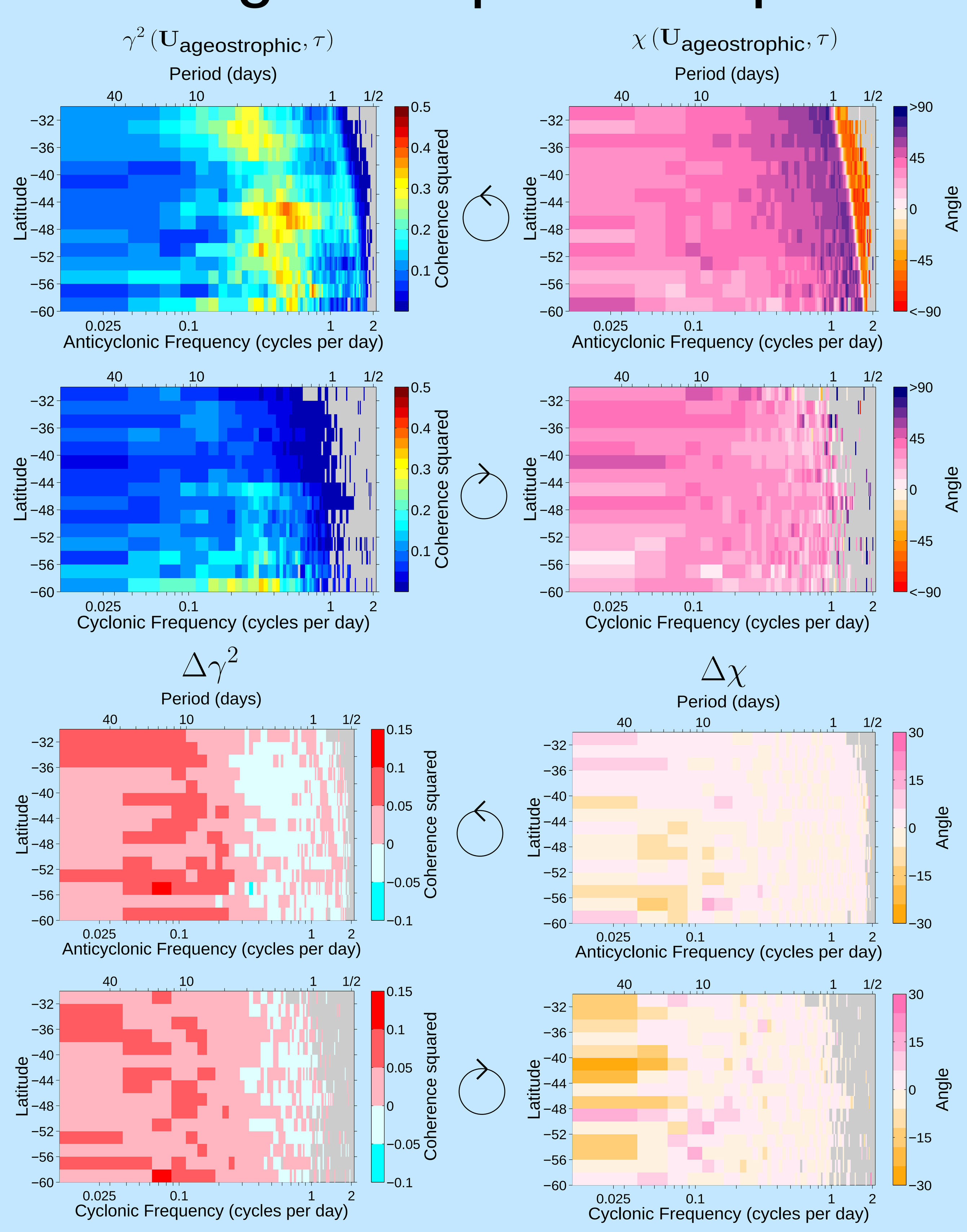

In order to estimate the wind-driven Ekman-type velocities from drifter observations we conducted cross-spectral analyses first between the drifter velocity and wind stress and second between the ageostrophic velocity and the wind stress.
► The **coherence squared** and **coherence phase** between the ageostrophic velocity and the wind stress are shown. Gray areas correspond to non statistically significant coherence squared at the 95% level.

► The highest γ^2 values are found for frequencies between 0.1 and 2 cpd between 42°S and 52°S corresponding to the latitudinal excursion of the core of the Antarctic Circumpolar Current.

► $\gamma^2 \geq 0.3$ corresponds to χ = 41.2°±0.4° on average. A maximum γ^2 of 0.38 is found for ν = 0.475 cpd (2.1 day period) and for the 44°S to 46°S latitude band with χ = 49.3°±0.1°.

► Higher γ^2 is found in the anticyclonic domain. In this same domain, χ changes sign at the inertial frequency. These results are in agreement with an Extended Ekman Theory which relates the Fourier components of the ocean velocity and of the wind stress through a linear function dependent on the frequency, the Coriolis parameter and the eddy viscosity [*Gonella, 1972*].

► These plots show the absolute variations $\Delta\gamma^2$ and $\Delta\chi$ from the case of conducting the wind stress cross-spectral analysis directly with the drifter velocity to the case of the ageostrophic velocity.

► $\Delta\gamma^2$ is up to +0.15 for frequencies lower than the AVISO maps Nyquist frequency. It means that non wind stress coherent velocity is successfully removed when subtracting the geostrophic velocity from the drifter velocity. This increase is significant because it is bigger than the errorbars for the coherence squared (less than 0.05) or variations due to a standard wind slip correction (not applied here).

► Zero coherence squared is found between geostrophic velocities and ECMWF wind stress (results not shown here)

6. Conclusions

► We showed (section 4) that geostrophic velocities from altimetry explain about 60% of the drifter velocity variance in the Southern Ocean.

► We showed (section 5) that when a geostrophic velocity is subtracted from the drifter velocity, an ageostrophic velocity is recovered which is coherent with wind stress.

► We are currently working on the relationship between ageostrophic velocities at the surface and wind forcing in the Southern Ocean.

Combining altimetry and drifter measurements is shown to be useful to study wind driven surface currents.

References

AVISO/Altimetry. *AVISO User Handbook for Merged TOPEX/POSEIDON products*, edition 3.0 edition, 1996.

Gonella, J., 1971. A local study of inertial oscillations in the upper layers of the ocean. *Deep-Sea Research*, **18**, 775–788.

Gouretski, V. V. and K. Jancke, 1998. A new climatology for the world ocean. WHP SAC Tech. Rep. no. 3, woce report no. 162/98, WOCE Special Analysis Centre, Max-Planck Institute, Hamburg.

Smith, S. D., 1980. Wind stress and heat flux over the ocean in gale force winds. *JPO*, **10**, 709–726.

Drifter data provided by Peter Niiler of SIO.

ECMWF winds provided by the Data Support Section of the Scientific Computing Division at NCAR.

For further information and handouts see http://www-pord.ucsd.edu/~selipot.